Bridge Structures
Vol. 5, Nos. 2–3, June–September 2009, 109–118

Seismic design and seismic performance retrofit study for the Akashi Kaikyo Bridge

M. Okuda*, S. Fukunaga and K. Endo

Honshu-Shikoku Bridge Expressway Co., Ltd, Kobe, Hyogo-prefecture, Japan

Presented in this paper is the original seismic design and the seismic performance retrofit study against large-scale earthquakes of the Akashi Kaikyo Bridge. The Akashi Kaikyo Bridge is the world's longest suspension bridge and was completed in 1998. In the original seismic design, an inland near-field earthquake with large magnitude was not considered for the seismic design force. Although the bridge encountered the Hyogo-ken Nanbu Earthquake in 1995, it was not seriously damaged since the earthquake occurred during its construction. Therefore, a seismic performance retrofit study against large-scale earthquakes has been started. In the seismic performance retrofit study, site-specific large-scale earthquakes including inland near-field earthquakes were defined based on the latest seismological information. As a result, it was found that target seismic performance was ensured by taking some minor countermeasures.

Keywords: Akashi Kaikyo Bridge; large-scale earthquake; seismic performance

1. Introduction

The Akashi Kaikyo Bridge is the world's longest suspension bridge with the total length of 3911 m, including the main span of 1991 m, as shown in Figure 1. This bridge was opened to traffic in April 1998, linking the Kobe City and the Awaji Island on the Honshu–Shikoku Expressway, which connects Japanese two major islands, Honshu and Shikoku.

Although the bridge was designed based on specific design standards, an inland near-field earthquake with large magnitude was not considered for the design seismic force. In 1995, the Hyogo-ken Nanbu Earthquake, the most disastrous inland near-field earthquake in Japan, struck the bridge. But the bridge received no serious damage because it was undergoing construction. Therefore, seismic performance against inland near-field earthquakes remained as an important problem.

According to the latest findings, there is concern that a large-scale earthquake exceeding the original design seismic force would occur. On the other hand, the bridge is designated as a lifeline corridor for emergency transportation in case of large-scale earthquakes. Therefore, the Honshu–Shikoku Bridge Expressway Company Limited decided to execute a seismic retrofit work against large-scale earthquakes including inland near-field earthquakes. After performing the seismic performance retrofit study, it was found that the target seismic performance criteria were possibly ensured by taking some minor countermeasures.

This paper describes the original seismic design, the influence of the Hyogo-ken Nanbu Earthquake and seismic performance retrofit study for the Akashi Kaikyo Bridge.

2. Topographical and geological condition

The Akashi Strait is located between Kobe City on Honshu and Awaji Island. It has a minimum width of about 4 km and a maximum water depth of about 110 m in the centre part. Detailed investigation by sonic prospecting indicated the existence of northeast–southwest faults as shown in Figure 2. Although there was no concrete evidence for those faults to move in the Quaternary period, the foundations were decided to be placed to avoid these faults.

The geological formation of the Akashi Strait consists of, in a descending order, the Alluvium, the upper Diluvium, the Akashi stratum, the Kobe stratum and the granite formation, as shown in Figure 3. Since the upper surface of the granite is located deeper than 150 m below the sea level at the proposed site of main towers and anchorage on the Kobe side, the foundations at these sites had no option but to rely on either the Kobe stratum or the Akashi stratum. The Akashi stratum is composed of semi-consolidated gravel and

*Corresponding author. Email: motoi-okuda@jb-honshi.co.jp

ISSN 1573-2487 print/ISSN 1744-8999 online

DOI: 10.1080/15732480903142807
http://www.informaworld.com

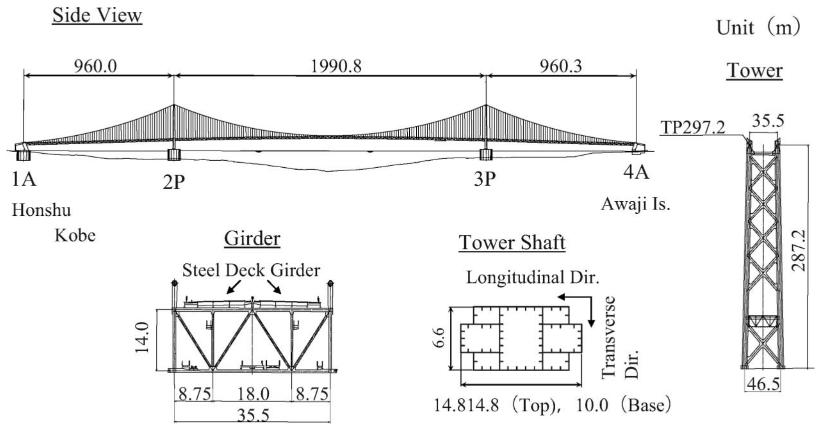

Figure 1. General view of Akashi Kaikyo Bridge.

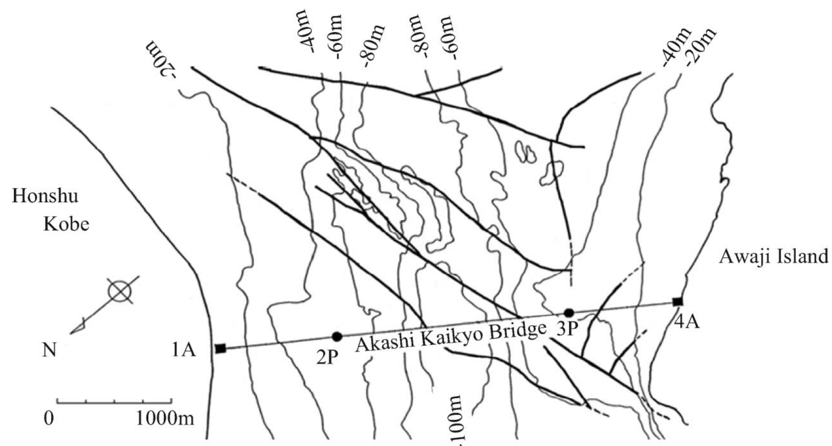

Figure 2. Topographical features and distribution of faults around the bridge.

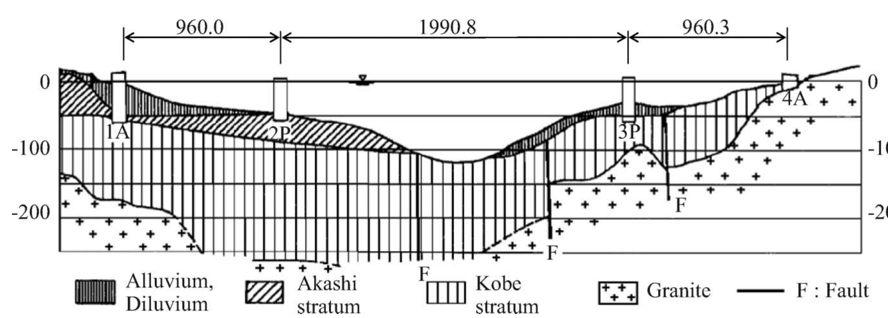

Figure 3. Geological formation of Akashi Kaikyo Bridge.

sand. The Kobe stratum is weakly cemented soft rock made of sandstone and mudstone layers.

3. Original seismic design

3.1. Original design seismic force

Japan is located in the earthquake-prone area, where plate boundaries and many inland active faults exist. Large-scale earthquakes with magnitude of about 8 on the Richter scale have occurred off the Pacific Coast, and medium-sized earthquakes due to inland active faults have happened around the bridge site.

Figure 4 shows acceleration response spectrum of original seismic design (Kawaguchi *et al.* 1987).

Acceleration response spectrum (damping coefficient: $h = 0.05$) of the design seismic motion for short period was determined as an envelope of the following two acceleration response spectra. They were

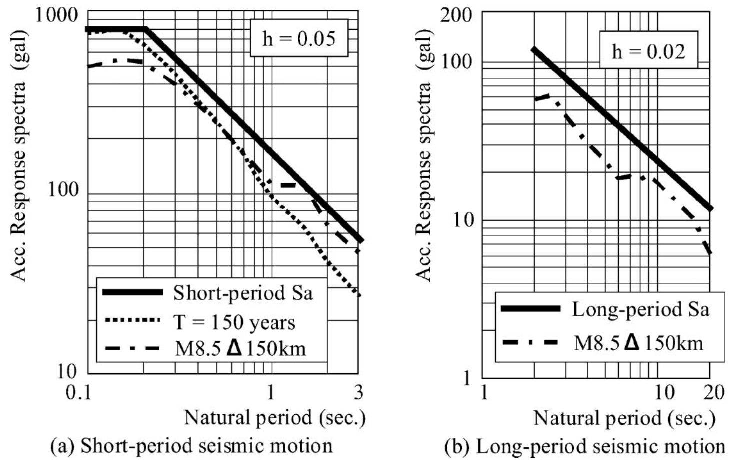

Figure 4. Acceleration response spectrum of original seismic design.

calculated by an attenuation equation by distance based on historical recorded seismic motions, assuming that the top surface of the Kobe stratum ($V_s = 600$–700 m/s) is exposed.

- One from a large-scale plate boundary earthquake whose magnitude and epicentre distance were assumed to be 8.5 on the Richter scale and 150 km, respectively.
- The other calculated by statistical theory based on historical recorded earthquakes around the bridge site (return period: $T = 150$ years).

Since the bridge has a very long natural period, design seismic motion for long period was also determined for superstructure. Acceleration response spectrum (damping coefficient: $h = 0.02$) of the design seismic motion for long period was determined by the same plate boundary type earthquake as for the short-period seismic motion. It was calculated by an attenuation equation by distance based on the records of seismographs for long-period seismic motions.

3.2. *Seismic analysis method*

Seismic analyses were performed for the substructure and the superstructure, respectively.

As the huge substructures were supported by relatively soft ground, they were designed considering soil–structure (kinematic) interaction, such as effective seismic motion and dynamic stiffness. The analyses were performed by the response spectrum method with two degrees of freedom rigid models against the short-period seismic motion.

The superstructure was designed against design seismic motions for both short period and long period. The analyses for the short-period seismic motion were performed by inputting effective seismic motions to respective foundations. The analyses for the long-period seismic motion were performed by inputting long-period seismic motions directly to the foundations and considering different arrival times of seismic wave at respective foundations with the speed of 1000 m/s. The analyses were performed by the time domain analysis method using modal analysis in the longitudinal direction and in the transverse direction, respectively. Responses of superstructure members were calculated by the square root of the sum of the squares of both 2/3 of smaller value and larger value out of both seismic responses in the longitudinal direction and the transverse direction.

3.3. *Seismic performance verification for substructure and superstructure*

Seismic performance of the substructures were verified by the safety factor for bearing capacity of 2.0, safety factor for sliding of 1.2 and eccentricity ratio of 0.206. Vertical seismic force was considered as one-third of maximum horizontal response acceleration for seismic performance verification of substructures. Seismic performance of the superstructures were verified by conventional allowable stress design method. The allowable stress during earthquake was 1.5 times that of allowable stresses in standard loading, which corresponded to about 88% of the yielding stress.

4. Influence of Kobe Earthquake

4.1. *Kobe Earthquake*

On 17 January 1995, an earthquake with a magnitude of 7.2 on the Richter scale occurred beneath the Akashi Strait, and its epicentre was very close to the Akashi Kaikyo Bridge. The earthquake caused extensive damage to Kobe City and about 6400 people lost their lives. At the time of the earthquake, the state of construction work of the Akashi Kaikyo Bridge was that erection of the main cables was just finished. Therefore, it was fortunate that erection of truss girder had not started.

4.2. *Influence by crustal movement*

Owing to careful inspection and survey carried out after the earthquake, it was found that the bridge received no serious structural damage. But the four foundations were moved due to the crustal movement by the earthquake, as shown in Figure 5. These movements were considered to be generated by the movement of faults which exist between the centre span from 2P to 3P, and the side span from 3P to 4A, as shown in Figure 2. As a result, the centreline of the bridge bent slightly; the span lengths between 2P and 3P as well as 3P and 4A were lengthened by 0.8 m and 0.3 m, respectively (Tada *et al.* 1995).

Safety of the bridge deformed by the earthquake was verified by performing various structural analyses based on the original design standard (Yasuda *et al.* 2000). Elongation of the span length was compensated by fabrication of the stiffening truss which was just underway. Two panels at the span centre and one end panel at 4A were extended by 40 cm and 34 cm, respectively so as to fit the new span length.

5. Seismic performance retrofit study

5.1. *Necessity for seismic performance retrofit*

In the original seismic design force of the Akashi Kaikyo Bridge, an inland near-field earthquake with large magnitude was not considered. According to recent promulgated earthquake information around the bridge site, there is concern that a large-scale earthquake exceeding the original seismic design force would occur. On the other hand, the bridge has to undertake a role of emergency transportation route in case of large-scale earthquakes. Therefore, the seismic performance retrofit study has been started for the bridge (Endo *et al.* 2009).

5.2. *Seismic performance retrofit study flow*

A flowchart of the seismic performance retrofit study is illustrated in Figure 6. In the study, several analyses that could simulate the nonlinear seismic behaviour accurately were performed by site-specific large-scale earthquakes in order to assess the seismic performance reasonably.

Since the bridge must undertake a role as an emergency transportation route in case of large-scale earthquakes, it is required not only to remain stable, but also to provide minimum operations and functions after earthquakes. Therefore, target seismic performance criteria were specified in terms of two aspects, seismic safety and serviceability. In terms of the seismic safety, the bridge must not collapse to ensure the life safety. In terms of the seismic serviceability after events, damaged structural members can be repairable, the serviceability for emergency traffic has to be ensured immediately after events by emergency inspections or temporary repair works and the serviceability for normal traffic has also to be ensured in a short period after events.

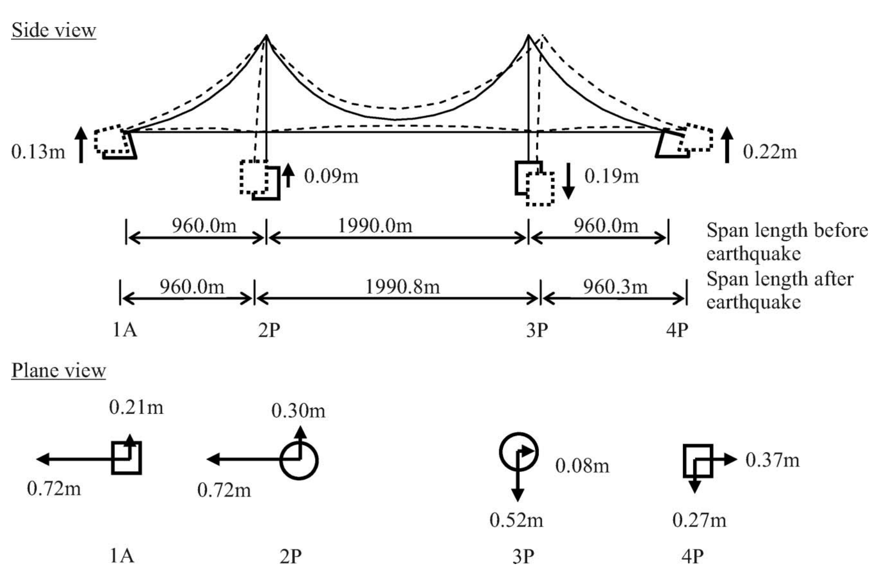

Figure 5. Displacement of foundations.

5.2.1. *Large-scale earthquake*

Owing to comprehensive fault surveys and various researches mainly performed after the Hyogo-ken Nanbu Earthquake in 1995, earthquake source information around the bridge site has become apparent. Besides, an estimation method of strong ground motions with fault models has been developed and practically used in some areas in Japan. Accordingly, it was decided that seismic ground motions of site-specific large-scale earthquakes were to be calculated with fault models based on the earthquake source information.

Figure 7 shows acceleration response spectrum of the seismic ground motions coming from the Rokko–Awaji Fault which is an inland near-field earthquake and Tounankai–Nankai Earthquake which is a plate boundary type earthquake. These are rock outcropping motions on the bedrock where S-wave velocity (V_s) is 2 km/s. A fault model of the Rokko–Awaji Fault is shown in Figure 8. In addition, another type of seismic ground motion coming from an unknown inland active fault with magnitude of 6.8 occurring just beneath the site were considered.

All the seismic ground motions were estimated by a hybrid method. The hybrid method provides wideband seismic ground motions by combining short-period seismic motions estimated by Green's function method and long-period seismic motions estimated by 3D finite difference method, etc. Green's function method is an artificially synthesising method of seismic motions of large-scale earthquake by adding seismic motions of small-scale earthquake spatially and temporally. The 3D finite difference method is an artificially synthesising method of seismic motions of large-scale earthquake by analytically calculating seismic motions due to fault rupture.

5.2.2. *Analytical model*

A three-dimensional full bridge model used for dynamic analyses is shown in Figure 9. Several

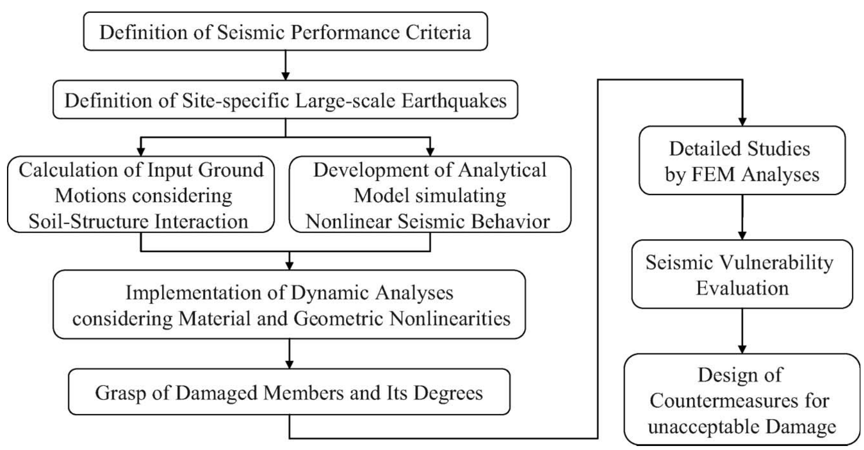

Figure 6. Flowchart of seismic performance retrofit study.

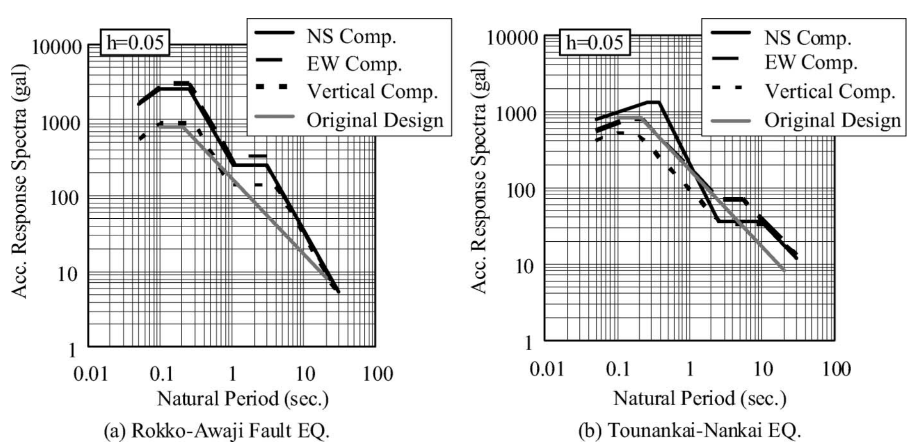

Figure 7. Acceleration response spectrum for seismic performance verification.

idealisations, which were able to simulate nonlinear seismic behaviours accurately, were incorporated in the analytical model based on the results of preliminary linear dynamic analyses. Each structural element was idealised as follows.

5.2.2.1. Tower and girder. Since the elements of towers and stiffening truss were subjected to bidirectional bending moments and axial force fluctuations, they were idealised by fibre elements, which were able to take into account those influences on material nonlinearity. Segmentalized cross-sections by fibre elements are shown in Figure 10. The constitutive law of these elements was assumed to be elastic-linear kinematic strain hardening model with 0.01E (where E is Young's modulus) as the second gradient. Members that got large sectional force in the preliminary analyses were divided into four or more elements between the joints as shown in Figure 9.

5.2.2.2. Main cable, suspender and stay rope. The cable members, such as main cables, suspender ropes and stay ropes, were idealised by linear beam elements of which flexural stiffness was almost zero. Cable behaviours, such as sagging due to the tension force

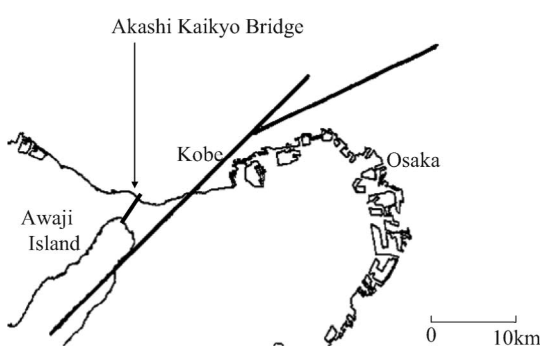

Figure 8. Fault model for the Rokko–Awaji Fault.

losing, were simulated by the fine segmentation of cable members (see Figure 9) as well as the implementation of geometric nonlinear analyses. Stay ropes, which restrain relative displacement between the girder and the main cable, are installed only in the centre span.

5.2.2.3. Foundation. Foundations were modelled as a rigid body, and nonlinear spring elements were installed at interfaces between the foundation and the ground in order to simulate its uplift and slip behaviours and yielding of the ground. The analytical model is schematised in Figure 11.

5.2.2.4. End link and tower link. End link supports the stiffening truss from below at the anchorage, and the tower link suspends the stiffening truss from above at the tower. The members were idealised by linear truss elements. Link behaviours were simulated by the implementation of geometric nonlinear analyses to reflect restoring characteristics, as shown in Figure 12.

5.2.2.5. Wind shoe and wind tongue. The girder is restrained in transverse direction by wind shoes attached to lateral trusses and wind tongues attached to horizontal beams at the tower position. This restraint was idealised by linear spring elements as schematised in Figure 13.

5.2.2.6. Pounding between girder and anchorage. Displacement of the stiffening truss of side span in the longitudinal direction is restrained by stoppers. A stopper of the stiffening truss for anchorage direction collides against the anchorage due to the excessive displacement in the anchorage direction, while the girder collides against a stopper for span direction due to the excessive displacement in the span direction. Nonlinear spring elements were installed at interfaces between the girder and the anchorage in order to

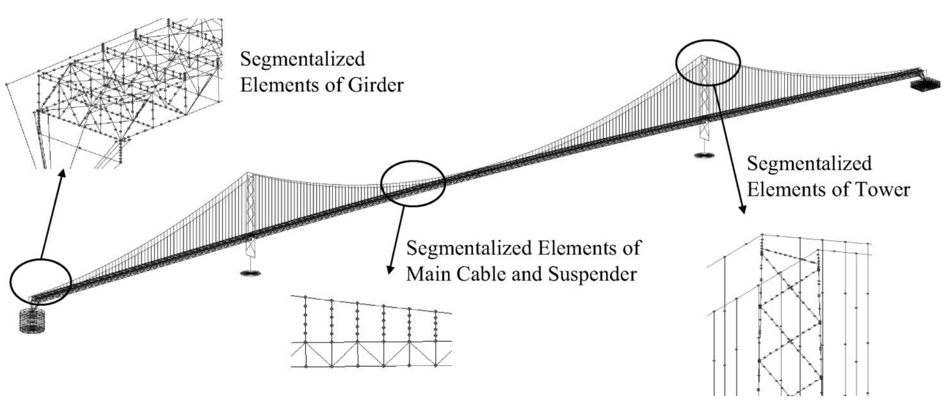

Figure 9. 3D full bridge model.

consider the pounding effect between those members. The analytical model is schematised in Figure 14.

5.2.2.7. Steel deck girder. Steel deck girder is supported by bearings on the stiffening truss. Steel deck girders were idealised by linear beam elements. Steel deck girder bearings were modelled as nonlinear spring elements in order to simulate its failure. The analytical model of steel deck girder bearing is shown in Figure 15.

5.2.2.8. Oil dampers. Effects of oil dampers between the girder and the tower, which were installed to improve aerodynamic stability of the tower in the original design, were incorporated in the full bridge analytical model using mass, spring and dashpot elements (see Figure 13).

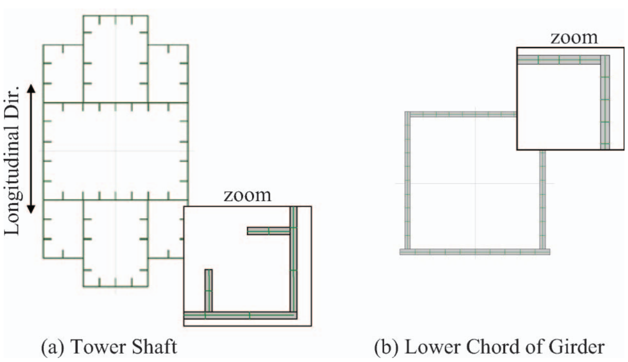

Figure 10. Analytical model of tower and girder.

5.2.3. *Analytical condition*

Nonlinear dynamic analyses taking into account both material and geometric nonlinearities were performed to simulate the seismic behaviours, since the suspension bridge is very flexible. As input motions into the analytical model, effective seismic motions considering soil–structure (kinematic) interaction were applied in three directions (longitudinal, transverse and vertical) simultaneously. Analytical conditions are as follows:

- Analytical method: time history response analyses with material and geometric nonlinearities.
- Numerical integration method: Newmark's β method ($\beta = 0.25$).
- Damping type: member based stiffness-proportional damping.
- Time interval: 0.0025 s.
- Damping ratios of members: 0.01 (tower, girder, cable), 0.10 (tower foundation), impedances calculated by soil–structure interaction analyses (anchorage foundation).

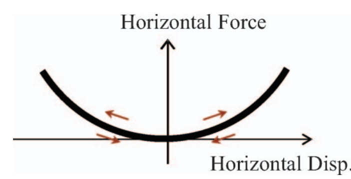

Figure 12. Force vs displacement relationship of tower link.

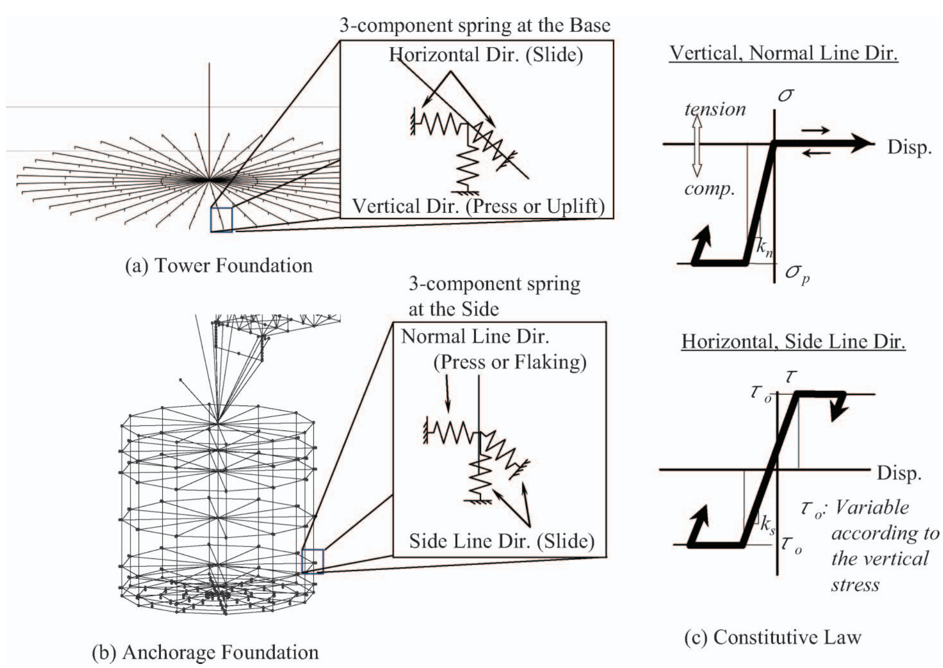

Figure 11. Analytical model of foundation.

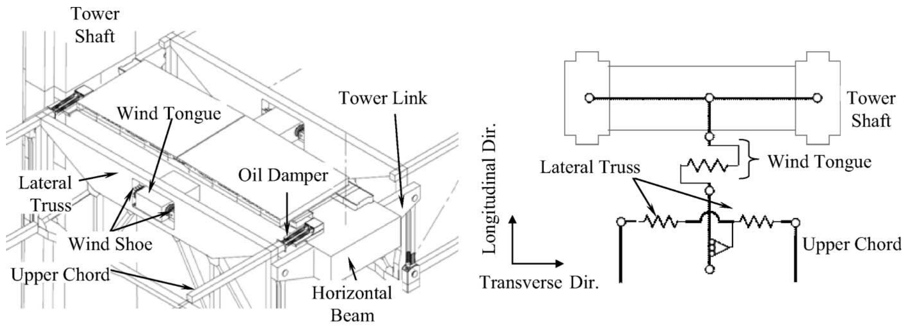

(a) Overview at connection between Girder and Tower (b) Installation of Spring Element

Figure 13. Analytical model of wind shoe and tongue.

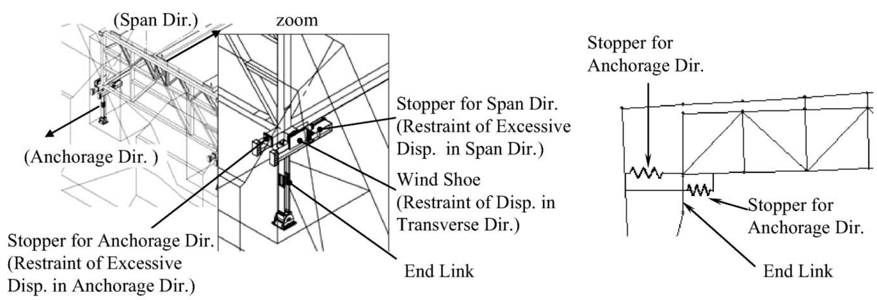

(a) Overview at Girder End (b) Installation of Spring Element

Figure 14. Analytical model of pounding effect.

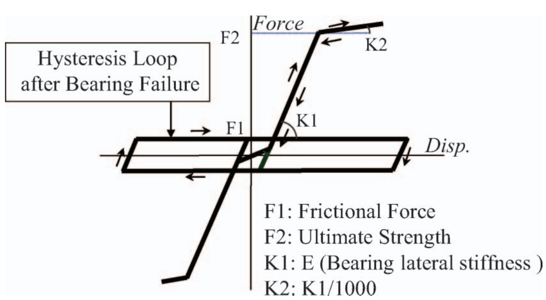

Figure 15. Analytical model of bearing failure effect.

5.2.4. *Analytical result and damage evaluation*

As responses to the Rokko–Awaji Fault Earthquake were dominant for the results among the three earthquakes, the results of Rokko–Awaji Fault Earthquake are described. Results of the seismic analyses are tabulated in Table 1. Although responses of the tower exceeded its buckling strength at the base of tower shafts and the lower horizontal beam, responses of other main structural elements, such as the main cable, suspenders and the girder were within elastic range. In addition, some damages at sub-structural elements, such as stoppers at the girder ends, bearings of the steel deck girder, expansion joints and oil dampers, were generated.

For the damage evaluation of the tower, detailed studies were performed by FEM analyses, which were pushover analyses using shell elements. Figure 16 shows the results of the lower horizontal beam. In terms of the M–θ relationship, flexural characteristics indicates almost linear until the maximum moment of the dynamic analysis and the structure has redundancy beyond the moment. In terms of the deformation diagram, the degree of local buckling by dynamic analysis moment is small enough to repair it. Furthermore, there is concern that strengthening of the horizontal beam might lead to the damage of the tower shaft, which is not desirable for the seismic performance of the entire bridge system. Therefore, the damage was assessed to be acceptable.

In addition, the damages of other sub-structural elements, such as stoppers at the girder ends, bearings of the steel deck girder and oil dampers, were also assessed to be acceptable, since the damages of those elements do not have much influence on operations and functions of the bridge and are repairable under traffic condition.

On the other hand, the damage of expansion joints was assessed to be not acceptable. Since expansion joints of the bridge are huge ones as shown in Figure 17, those failures might result in large holes, approximately 2.3 m long in the longitudinal direction, on the road surface. Accordingly, there is a fatal possibility that a

Table 1. Analytical results.

Structural member	Element	Results
Tower	Shaft at middle	Strain ratio (maximum response/buckling strength) = 0.98
	Shaft at base	Strain ratio (maximum response/buckling strength) = 1.03*
	Diagonal	Strain ratio (maximum response/buckling strength) = 0.76
	Upper horizontal beam	Strain ratio (maximum response/buckling strength) = 0.59
	Lower horizontal beam	Strain ratio (maximum response/buckling strength) = 1.42*
	Anchor bolt	Strain ratio (maximum response/buckling strength) = 0.59
	Base concrete	Strain ratio (maximum response/strength) = 0.98
Main cable	Cable	Tensile force ratio (maximum response/ultimate strength) = 0.45
	Slide at saddle	Minimum safety factor = 2.7
Suspender	Rope	Tensile force ratio (maximum response/ultimate strength) = 0.25
	Slip of cable band	Minimum safety factor = 1.7
Centre stay	Rope	Tensile force ratio (maximum response/ultimate strength) = 0.86
	Slip of cable band	Minimum safety factor = 1.1
Girder	Upper and lower chord	Strain ratio (maximum response/buckling strength) = 0.81
	Diagonal	Strain ratio (maximum response/buckling strength) = 0.52
	Lateral	Strain ratio (maximum response/buckling strength) = 0.82
	Pounding at anchorage	Pounding*
	Pounding at tower	No pounding
	Stopper	Axial force ratio (maximum response/yielding strength) = 1.29*
Steel deck	Bearing	Failure at some bearings*
Link	Tower link	Axial force ratio (maximum response/yielding strength) = 0.44
		Displacement ratio (maximum response/allowable value) = 0.26
	End link	Axial force ratio (maximum response/yielding strength) = 0.54
		Displacement ratio (maximum response/allowable value) = 0.19
Wind shoe (tongue)		Horizontal force ratio (maximum response/yield strength) = 0.93
Expansion joint		Failure at tower on side span side*
Oil damper		Failure at all dampers*
Foundation	Stability	Minimum safety factor = 1.1

*Some damage or nonlinear behaviour was developed.

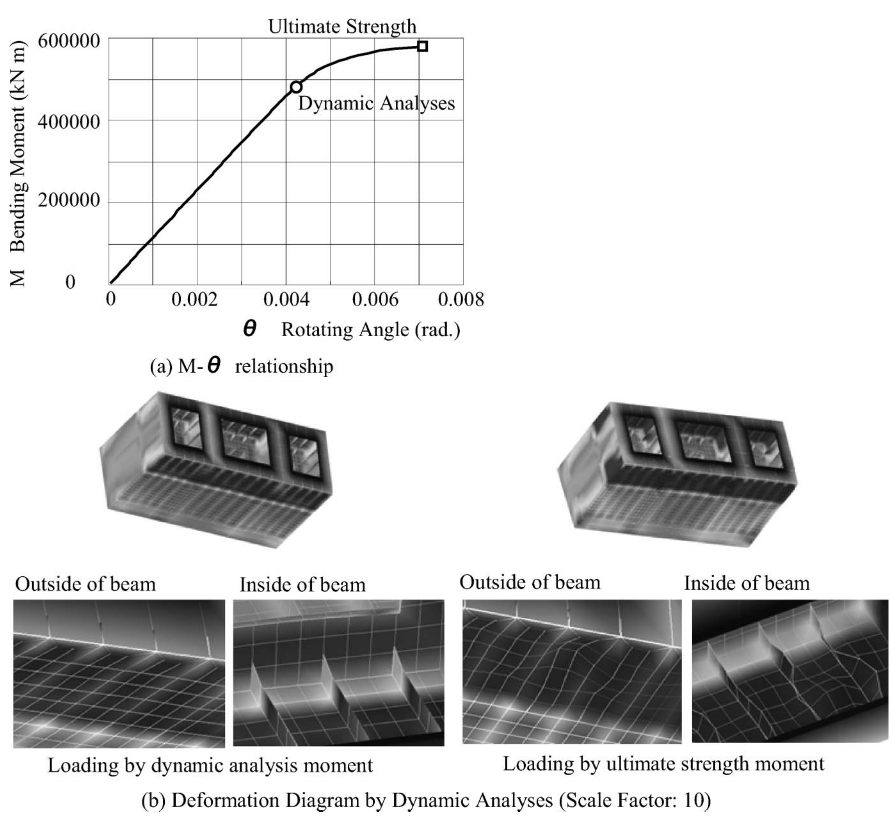

Figure 16. FEM analyses of lower horizontal beam.

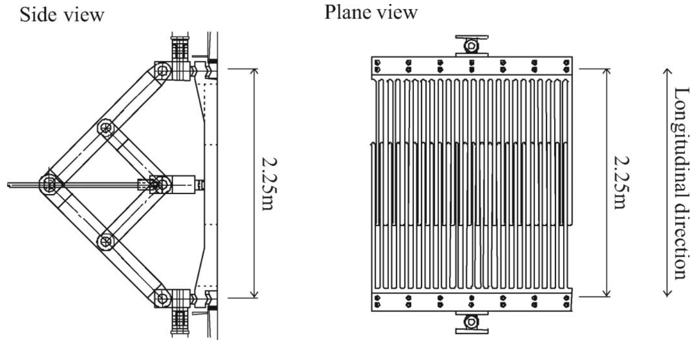

Figure 17. Expansion joint at tower.

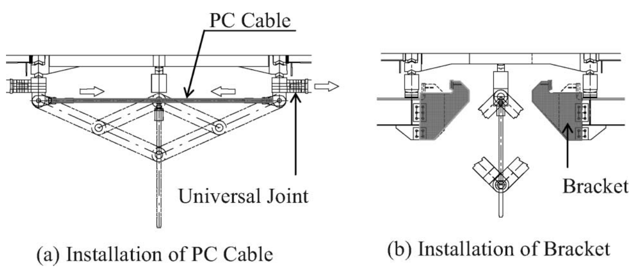

Figure 18. Planned retrofit measures.

vehicle might fall from a 80-m height during an earthquake. A planned countermeasure for the expansion joints is shown in Figure 18. PC cables aim to lead failure to a universal joint when the expansion joints spread beyond its allowable range, while brackets aim to support the expansion joints vertically after the universal joints fail.

6. Conclusions

This paper presented the original seismic design, the influence of the Hyogo-ken Nanbu Earthquake and the seismic performance retrofit study of the Akashi Kaikyo Bridge. In the original seismic design, an inland near-field earthquake with large magnitude was not considered for the design seismic force. The bridge was completed overcoming initial deformation caused by crustal movement due to the Hyogo-ken Nanbu Earthquake. As it was assumed that a large-scale earthquake exceeding the original design seismic force would occur, it was decided to perform a seismic performance retrofit study. Seismic ground motions of site-specific large-scale earthquakes were estimated by a hybrid method using fault models. After performing nonlinear dynamic analyses with a 3D full bridge model and FEM analyses with shell models, it was found that most of the structural elements were sound and the target seismic performance criteria were possibly ensured by taking some minor countermeasures even though the seismic force got larger. The primary reason for this result seems to be that effects of earthquake were not dominant load combination for most of the structural elements in the original design and there were some margins against an earthquake. In order to provide safe transportation of the Akashi Kaikyo Bridge during a large-scale earthquake, the retrofit works are scheduled to be conducted in a few years.

References

Endo, K., *et al.*, 2009. Seismic performance verification of the Akashi-Kaikyo Bridge against large-scale earthquakes. *In*: *Sixth International Conference on Urban Earthquake Engineering*, 3–4 March 2009, Tokyo, Japan.

Kawaguchi, K., *et al.*, 1987. Earthquake resistance design of Akashi Kaikyo Bridge. *In*: *3rd Workshop on Performance and Strengthening of Bridge Structures*, 8–9 May 1987, Tsukuba, Japan.

Tada, K., *et al.*, 1995. Effect of the southern Hyogo Earthquake on the Akashi–Kaikyo Bridge. *Structural Engineering International*, 5, 179–181.

Yasuda, M., *et al.*, 2000. Seismic design and behavior during the Hyogo-ken Nanbu Earthquake of the Akashi Kaikyo Bridge. *In*: *12th World Conference on Earthquake Engineers*, January 2001, Auckland, New Zealand.